

Skyhook-PID Controller for Active Railway Pantograph

Munaliza Ibrahim¹, Mohd Azman Abdullah^{1,2,*}, Mohd Hanif Harun^{1,2},
Fathiah Mohamed Jamil¹, Fauzi Ahmad^{1,2}

¹Faculty of Mechanical Technology and Engineering, Universiti Teknikal Malaysia Melaka,
Hang Tuah Jaya, 76100 Durian Tunggal, Melaka, Malaysia

²Centre for Advanced Research on Energy, Universiti Teknikal Malaysia Melaka,
Hang Tuah Jaya, 76100 Durian Tunggal, Melaka, Malaysia

*Author to whom correspondence should be addressed:

E-mail: mohdazman@utem.edu.my

(Received December 4, 2023; Revised February 26, 2024; Accepted June 21, 2024).

Abstract: This article describes a technique for an active pantograph in rail transportation using two different active control technologies to control the vertical displacement between the railway pantograph and the overhead contact line. The performance of proportional-integral-derivative (PID) controllers and skyhook PID controllers based on disturbances such as step, sinusoidal, and random inputs was investigated. Active traction pantograph systems with Skyhook PID controllers show better performance than passive pantograph systems by Root Mean Square (RMS) analysis. In summary, this simple skyhook PID controller can be proposed for future experimental approach of active railway pantograph.

Keywords: PID controller; Skyhook-PID controller; pantograph model; active pantograph

1. Introduction

Nowadays, rail vehicle systems are electrically powered. The current is transmitted from an overhead line system to the rail vehicle via a mechanical arm, the so-called current collector, as shown in Fig.1. The effectiveness of a current collection system and the stability of the interaction between the overhead contact line and pantograph are two factors that influence the performance of a high-speed train¹. This electrical collection system detects variations in contact force when a train is moving at high speed. The pantograph must remain in contact with the contact wire. If contact is interrupted, the repeated changes in the level of contact force caused by disconnecting and reconnecting the pantograph to the wire will generate sparks, which will affect the efficiency of the electrical collection system². This is mainly due to the fact that reliable current collection ensures both the safety and stability of high-speed train operation and is a prerequisite for train acceleration³. To maintain consistency, this tactile force variation must be under control.

One of the crucial phases in the design of an active railway pantograph is the pre-design. Most often, numerical and analytical methods are used to develop the initial design. Comparing modeling and simulation to an experimental process, there are many advantages⁴. However, creating a computational model that analyses

and predicts the short-term, dynamic behavior over time of a complex system is usually a big undertaking and a time-consuming process. It is crucial to have knowledge of how to set up a network connection and how to integrate all physical properties into the modelling. Modeling involves creating a representation that reflects the key characteristics of an actual system⁵. Constructing such a simulation enables analysts to foresee how modifications may impact the system's operations and outcomes. According to recent technological developments, a modeling and simulation environment can be used to represent a vehicle's behavior¹¹. For scientists and engineers, simulation is a crucial tool in the development process. Researchers studying the dynamic behavior of vehicles are increasingly interested in the disciplines of modeling and simulation. Compared to other methods, they are fast and unambiguous methods for assessing how the vehicle's handling and maneuverability characteristics respond in real-time operating conditions.

Verification is a step in any simulation study that compares two or more results to ensure their accuracy. In this study, the model implementation and the associated data are compared to the commercial software called Algodoo. Algodoo, a 2-dimensional physics-based simulation software is used as a verification technique due to its user-friendly interface and its unique position among

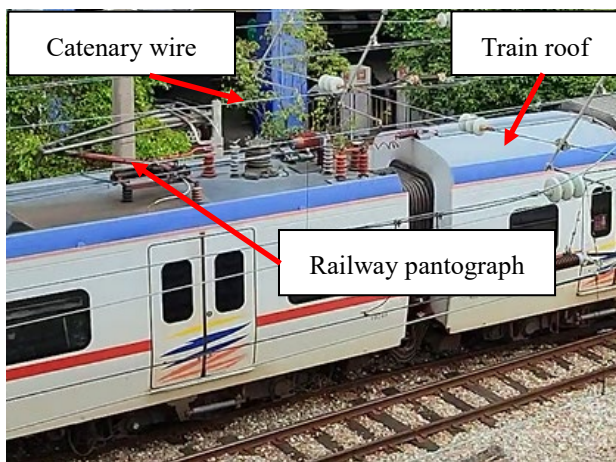


Fig. 1: The railway pantograph and catenary wire system.

serious computer modeling and computer games⁶). With an easy-to-use and aesthetically pleasing motion and animation interface, Algodoo is an open-source program originally developed for math classes. Phun, the first iteration of Algodoo, was made available in 2008 as an educational tool, a multifunctional software platform for game design, animated media creation, and technical engineering applications with flexible capabilities⁷.

Active pantographs are a typical strategy to enable current collection quality or to reduce wear on the catenary. Recent research proceeding active pantographs has focused mainly on the controller method used on the first high-speed trains⁸). Various PID controller schemes for the pantograph and other applications have also been introduced by many researchers⁹⁻¹¹). A deep reinforcement learning (DRL) to overcome the complex time-varying characteristic of Pantograph Catenary System by using finite-frequency H-infinity and multi-objective robust control (MORC) strategy¹²). A LQR controller and a methodical optimization procedure were used for pantographs of light railway vehicles¹³). A fuzzy-PID controller using an LMI (Linear Matrix Inequalities) control approach has also been demonstrated by a few researchers¹⁴). A self-adjusting, fuzzy logic-based control system of type 2, employing the Moradi-Zirhoi-Lin type-reduction technique, was effectively developed and deployed¹⁵). While the rate function was introduced into neural adaptive control for robust adaptive output feedback control¹⁶). There was a genetic algorithm PID controller introduced by a researcher for pantograph catenary system with model order reduction¹⁷). The controller designed for a pantograph catenary system should have three key characteristics, including ease of implementation and tuning, flexibility in the face of uncertainties and disturbances, and optimal performance assurance.

In this article, a simple three-degree-of-freedom (3DOF) pantograph model is verified using two-dimension (2D) physics-based simulation software. The outcomes of simulations evaluating active control approaches are provided and the implementation of

adaptive control techniques for a train pantograph is analyzed. The aim is to enhance contact stability in the dynamic interaction between the pantograph mechanism and catenary line. This study examines the performance of Proportional-Integral-Derivative (PID) and Skyhook-PID controllers for the vertical displacement of a railroad pantograph model. Pantograph performances are compared between PID, Skyhook-PID and passive controls with input disturbances of 0.01 meter, sinusoidal wave with an amplitude of 0.01 meter and an angular frequency of 2π radians per second and a random height disturbance of 0.01 meter. Based on the disturbances, the passive and active vertical displacement behavior of the pantograph model was examined. A simple tuning procedure is used to attain the optimum value of the PID controller¹⁸). A relative study by Root Mean Square (RMS) analysis was performed between active systems with PID and Skyhook-PID controllers for vertical displacement and passive systems. The research paper introduces the concept of active displacement control, which aims to reduce the vertical displacement of 3DOF railway pantograph systems. Excessive displacement can lead to problems such as reduced contact quality, increased component wear, and lower energy efficiency.

2. Railway pantograph model verification

The railway pantograph is assessed in this section through the use of some statistical tests to measure the mean relative absolute error and treating the model with a visual technique by comparing the tendency of the simulation results with those of other commercial software such as Algodoo and using the same input signals.

2.1 Railway pantograph modeling in Algodoo

As shown in Fig. 2, the pantograph model has been simplified to a 3DOF system consisting of three concentrated masses - the mass of the contact strip, the mass of the pan head, and the mass of the other pantograph components except for the contact strip and pan head. In general, the linearization of the nonlinear equation of motion of the frame at a certain height can be used to determine the lumped mass of the frame. Taking this into account, a simplified linear representation of the pantograph model is developed, consisting of the damper and the spring as mass. This model can accurately define the vertical motion of the pantograph is analyzed by taking into account only the gravitational forces acting on the masses.

The component of the catenary wire is depicted by a simple spring and damper for analysis. Initially, only the weights of the masses affect the motions. Due to the software constraint to produce such inputs, the bottom support of the pantograph is modified to a rotational part (Fig. 2a). The inputs are assumed directly from the track to the body to the pantograph support. The input moves and hits the support at a certain force. Figure. 2b show the

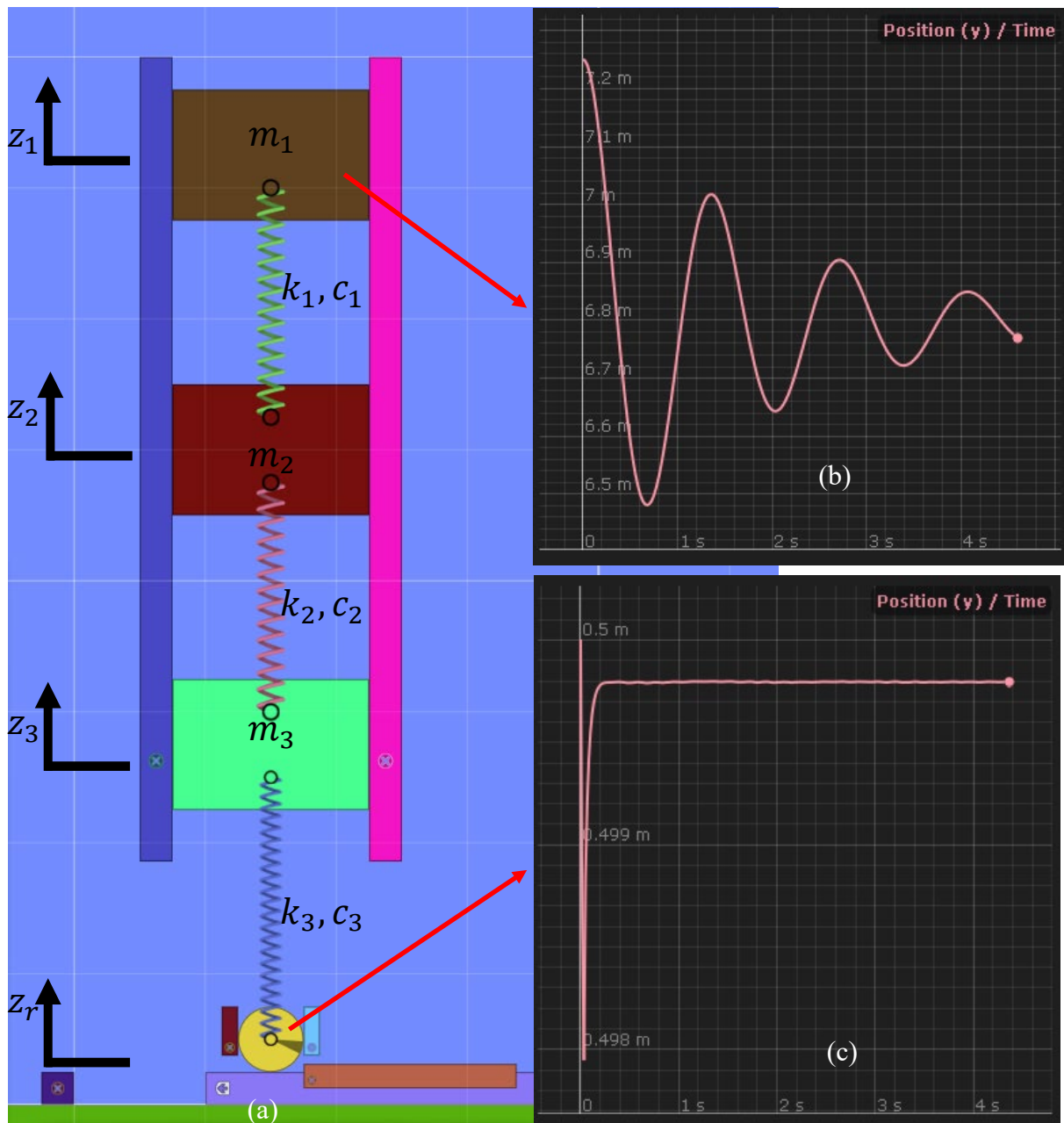


Fig. 2: (a) Pantograph simulation in Algodoo. (b) Response at z_1 . (c) Response at z_r .

Table 1. The parameter of the pantograph¹⁹.

Parameter	Value	Units
m_1	12	kg
m_2	5	kg
m_3	10.38	kg
k_1	32992	N/m
k_2	14544	N/m
k_3	611.85	N/m
ξ_1	0.1	-
ξ_2	0.1	-
ξ_3	0.1	-

responses at z_1 and Fig. 2c show the responses at z_r when the weights of the masses affect the motions. The physical parameters of the railway pantograph are listed in Table 1 with the damping ratios equal to 0.1. This study used a combination of MATLAB/Simulink based on the zero-dimensional model to build the railway pantograph model according to the mathematical equations below. The model should include the input z_r from Algodoos as the disturbance to generate the output of vertical displacement z_1 . The damping ratio is expressed as,

Consequently, the equation for the damping ratio should be expressed as,

$$\xi = \frac{c}{2\sqrt{km}} \quad (1)$$

where ξ represents the damping ratio, c is the damping coefficient, k is the spring stiffness constant, and m is the mass of each component.

2.2 Railway pantograph modeling in MATLAB/Simulink

The railway pantograph is a device that is usually positioned on top of a rail vehicle. As shown in Fig. 3 as a physical model of the pantograph, the purpose of the pantograph is to raise the railway pantograph to the appropriate working altitude so that it can contact the catenary wire and transmit the electricity. In general, a pantograph consists of contact strip, pan head, upper arm, lower arm, forth bar, base, air cylinder and control box.

To understand the dynamic behavior of the pantograph catenary system, the catenary model is crucial. The catenary can be modeled using a variety of approaches for a variety of reasons. There are mainly two types of modeling techniques. In the first method, the catenary's equations of motion are formulated using the structural modes as generalized coordinates. This technique is very useful for accurate catenary modeling in a variety of applications. It is mainly used for simple catenary systems, as it performs poorly when addressing complex catenary systems. The second way reduces the complexity of the structure and an analytical or numerical model of the catenary can be developed. The second approach is simple and can produce useful results. This study uses the catenary as a simple catenary model composed of suspension wires, contact wires, hangers, supports and limiters.

The pantograph is depicted in a simplified spring-mass model, consisting of three lumped masses representing the contact strip (m_1), pan head (m_2), and the remaining pantograph components such as the upper arm, lower arm, and base frame represented by m_3 . Spring-damper elements connect m_1 and m_2 , m_2 and m_3 , as well as m_3 and the base. The equation of motion for the contact strip is given by Equation 2, the pan head by Equation 3, and the mass m_3 by Equation 4. Therefore, the governing dynamic

equilibrium equations for the railway pantograph system can be written as,

$$m_1\ddot{z}_1 = k_1(z_2 - z_1) + c_1(\dot{z}_2 - \dot{z}_1) \quad (2)$$

$$m_2\ddot{z}_2 = -k_1(z_2 - z_1) - c_1(\dot{z}_2 - \dot{z}_1) + k_2(z_3 - z_2) + c_2(\dot{z}_3 - \dot{z}_2) \quad (3)$$

$$m_3\ddot{z}_3 = -k_2(z_3 - z_2) - c_2(\dot{z}_3 - \dot{z}_2) + k_3(z_r - z_3) + c_3(\dot{z}_r - \dot{z}_3) \quad (4)$$

2.3 Damping parametric analysis

Some damping coefficients exhibit nonlinearity in their data. Since the model is inherently linear, a procedure was required to linearize this data, which was applied iteratively to correct the values for each input. To assess the sensitivity of the predicted responses to parameter errors, a parametric analysis of damping was performed. Statistical errors, such as the mean absolute relative error and its percentage, were used in the analysis to assess the accuracy or error of the model.

The mean relative absolute error ($\bar{\varepsilon}$) can be calculated using Eq. 5 and Eq. 6 while as Table 2 shows the range of damping ratio used to find the optimal damping ratio at the lowest error in the pantograph model.

$$\varepsilon_i = |x_{A,i} - x_{M,i}| \quad (5)$$

$$\bar{\varepsilon} = \frac{\sum_{i=1}^n |x_{A,i} - x_{M,i}|}{n} \quad (6)$$

where ε_i refers to error values between Algodoos model and Matlab/Simulink model while as $\bar{\varepsilon}$ is the mean relative absolute error and n is the total set of data used in the simulation. As can be seen from Fig.4 to 6, the damping parameter analysis is obtained for each damping ratio.

Figure 7 shows the reactions of the contact strip displacement z_1 during mass movement. It can be seen that due to the influence of tension and gravity due to the mass motion, the minimum time to reach initial equilibrium should be greater than 10 s. A comparison of the simulation results from the Simulink and Algodoos models shows their responses are almost equal, with the mean relative absolute error between the models being 0.0017 and the percentage displacement error is 0.17%

Table 2. Range of damping ratio.

Parameter	Damping ratio	Optimal damping ratio	$\bar{\varepsilon}$	Damping coefficient
c_1	0.1 - 0.2	0.19	0.0017	2642.6779
c_2	0.1 - 2.0	0.1	0.0017	539.3329
c_3	0.1 - 3.0	2.1	0.0018	30.2834

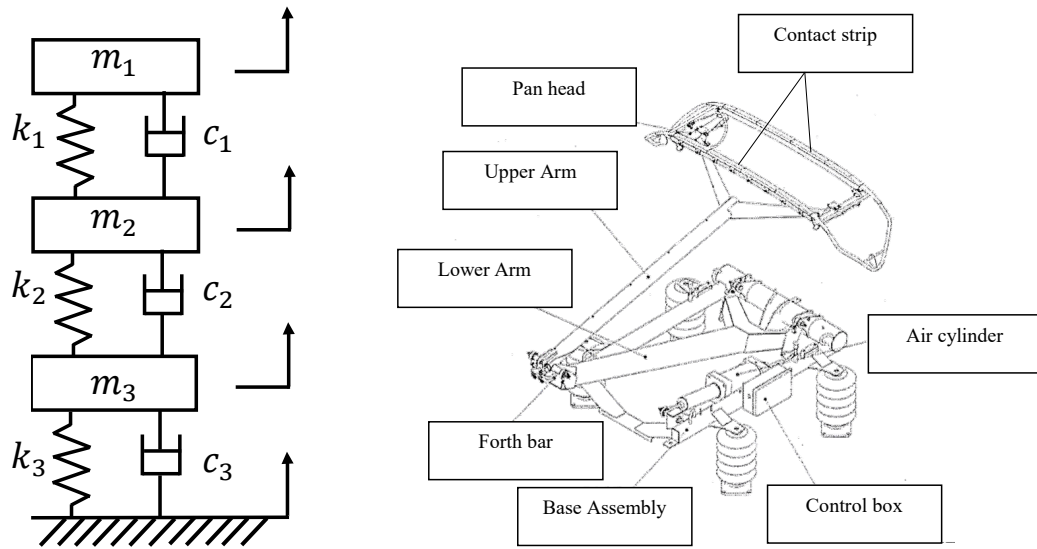


Fig. 3: Physical model of the railway pantograph.

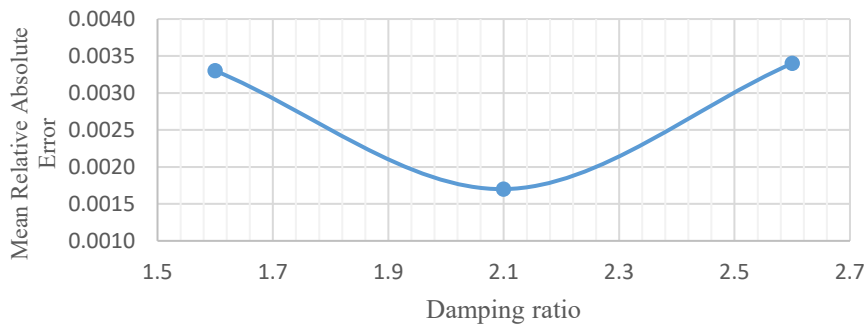


Fig. 4: Damping parametric analysis for c_1 .

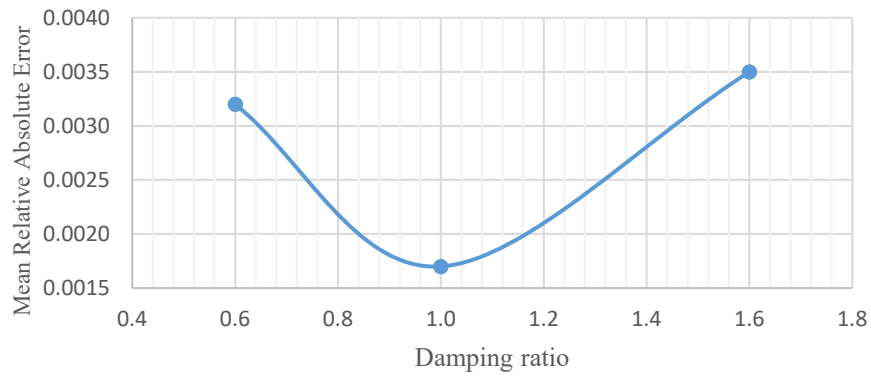


Fig. 5: Damping parametric analysis for c_2 .

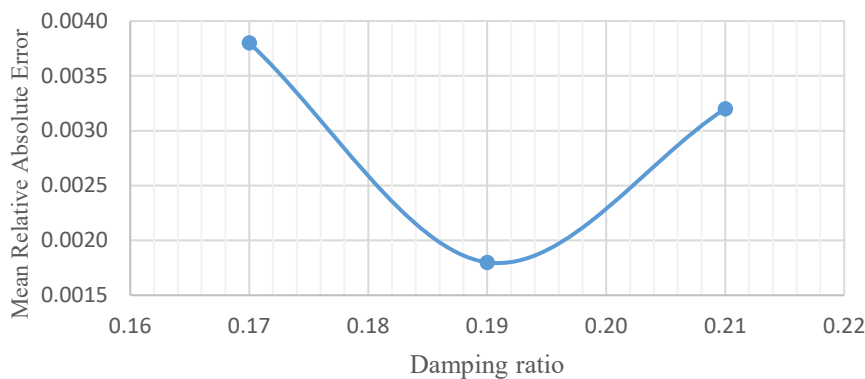


Fig. 6: Damping parametric analysis for c_3 .

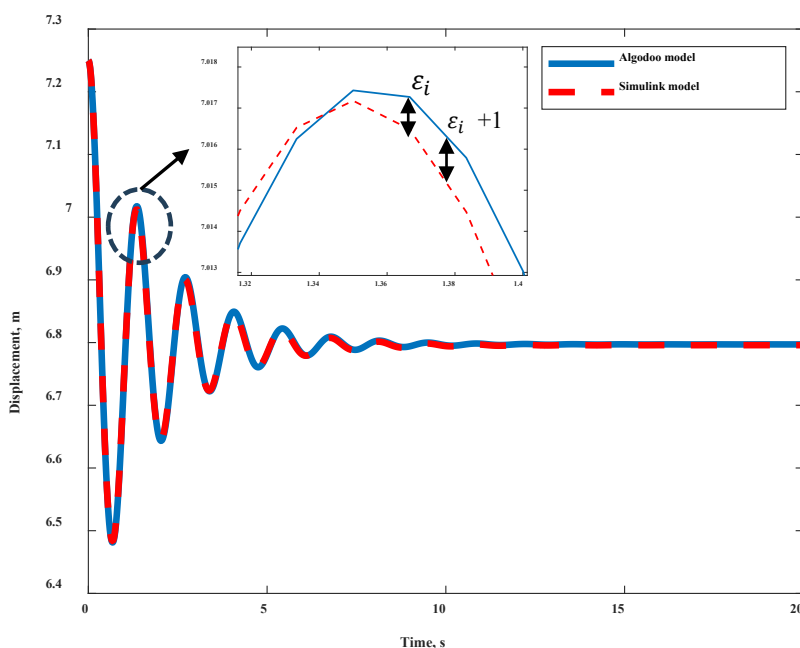


Fig. 7: Output responses of contact strip vertical displacement.

3. Controller design methods

Requirements design assignment is important before starting any design approaches. Current collection systems must react quickly and without overshoot.

3.1 Active pantograph control model

As previously stated, the objective of implementing active pantograph control is to enhance the dynamic performance of the pantograph-catenary engagement. Specifically, it aims to minimize variations in contact force that result when a pantograph passes over the catenary at high velocities. Figure.8. below is the physical model of the active pantograph with attachment of f_a as a force of an actuator. The system was given a step input of 0.01 meter at sample time 0.01 second, a sinusoidal input

of 0.01 sinusoidal amplitude at a frequency of 2π rad/s, and a random input ranging from -0.01 meter to 0.01 meter. Next, the pantograph dynamic equilibrium equations for the active system should be written as Eq. 7 below.

$$m_3 \ddot{z}_3 = -k_2(z_3 - z_2) - c_2(\dot{z}_3 - \dot{z}_2) + k_3(z_r - z_3) + c_3(\dot{z}_r - \dot{z}_3) + f_a \quad (7)$$

3.2 PID controller

The control methods used in the railway pantograph system are usually simple control mechanisms such as PID controllers^{20,21}. A simple method PID controller tuning technique was utilized. The controller parameters were automatically adjusted to counteract disturbances. The optimal P, I, and D values determined for the system are provided in Table 3.

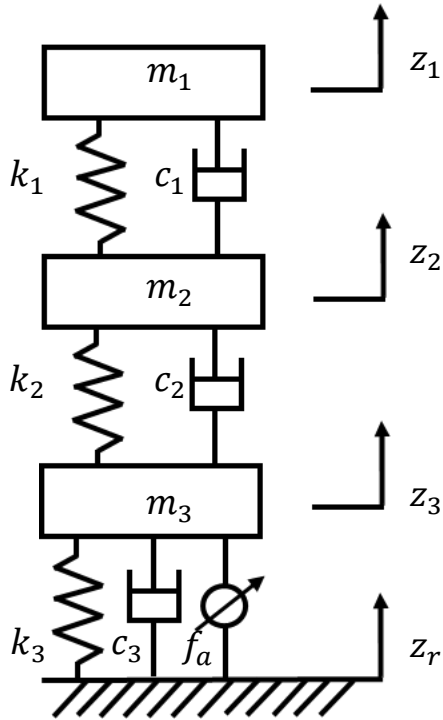


Fig. 8: Physical model of the Active pantograph.

3.3 Skyhook- PID controller

The skyhook control method has been extensively and successfully implemented across a variety of mechanical applications^{22,23}. It is derived from an imaginary damper attached in the sky²⁴⁻²⁶. The skyhook equation is expressed in Eq. 8,

$$F_{sky} = c_{sky}[\alpha(\dot{z}_r - \dot{z}_3) - (1 - \alpha)\dot{z}_3] \quad (8)$$

where, c_{sky} is the damping coefficient of the virtual skyhook, $\dot{z}_r - \dot{z}_3$ is velocity of the sprung mass while as, α is the magnitude of the control gain. The best combination of the Skyhook P, I, and D values depicts in Table 4 below.

3.4 Performance analysis method

In statistics, the root mean square (RMS) is defined as the square root of the mean of the squares of a dataset. It is a specific case of the generalized mean with an exponent of 2, also referred to as the quadratic mean. To assess the simulation results, RMS metrics are utilized. The RMS is calculated using the following formula for a group of N values $x_1, x_2, x_3, \dots, x_n$ can be calculated using Eq. 9. The percentage of improvement between both system passive and active was determined using Eq. 10.

$$x_{RMS} = \sqrt{\frac{(x_1^2 + x_2^2 + x_3^2 \dots + x_n^2)}{N}} \quad (9)$$

$$\% \text{ improve} = \left| \frac{\text{offset}_{passive} - \text{offset}_{active}}{\text{offset}_{passive}} \right| \times 100 \quad (10)$$

4. Results and discussion

Fig. 9-11 compare results between active railway pantograph with PID controller, Skyhook-PID controller, and passive system. The solid red line shows the passive system response. The blue dashed line represents the active system with PID control. The active Skyhook-PID control is the green dashed line. The optimal controller discussed above with the values of K_P , K_I , and K_D as mentioned in Table 3 and Table 4 then shows the performance of the active controller.

Table 3. The best combination of P, I, D values.

Constant	Step	Sine	Random
K_P	0	1	1
K_I	350.5404	350.5404	350.5404
K_D	0	1000	1000
Filter coefficient (N)	100	100	100

Table 4. The optimal Skyhook- PID controller parameter values of P, I and D

Constant	Skyhook- PID
K_P	37.7906
K_I	1194.2535
K_D	-0.3384
Filter coefficient (N)	88.6537

4.1 Step input

Figure 9 shows the vertical displacement at z_1 for each system when disturbed by the step input. The numerical simulations demonstrate that implementing this control system decreases the vertical motion of the contact point.

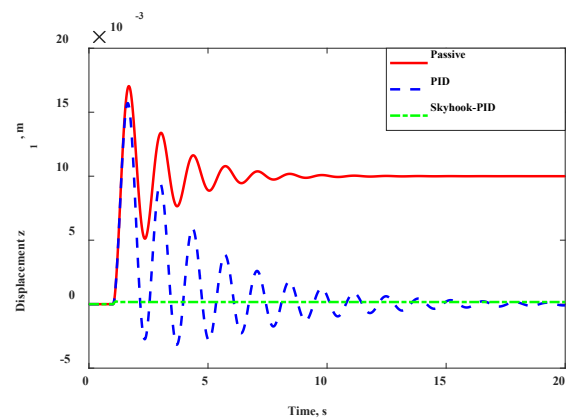


Fig. 9: Output responses of contact strip vertical displacement for step input.

4.2 Sine input

Figure 10 below shows the vertical shift in z_1 for each system when perturbed by the sine input. It can be seen that controller action substantially dampens shift value oscillations, evidenced by increased minimums and

decreased maximums. For minimizing displacement fluctuations, the Skyhook-PID controller demonstrates superior control performance compared to the standard PID controller.

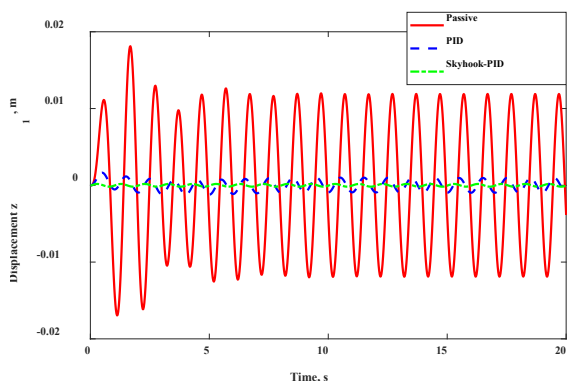


Fig. 10: Output responses of contact strip vertical displacement for sine input.

4.3 Random input

Figure 11 shows the vertical shift at z_1 for each system when perturbed by the random input. This study shows that the proposed Skyhook PID controller can well control the pantograph's dynamic response by minimizing the variance of the contact force. As a result, they prevent wear on the contact wire and pantograph contact strips and ultimately improve the current collection.

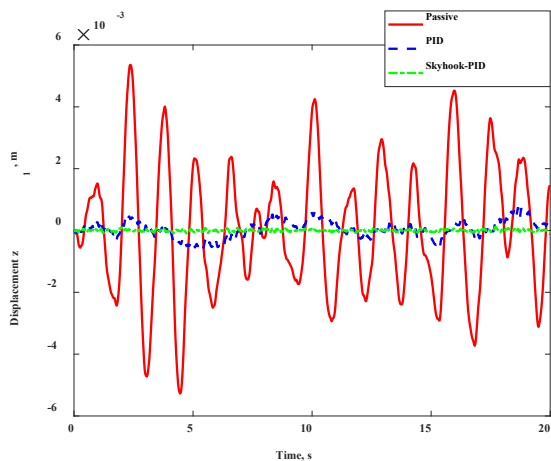


Fig. 11: Output responses of contact strip vertical displacement for random input.

4.4 Controller performance analysis

Table 5 summarizes the numerical results in terms of RMS values and percentage of improvement for step, sine, and random input for each system. Note that the lower RMS values indicate a better fit for the proposed controller. Although the displacement improvement is small, the contact quality has noticeably improved relative to the uncontrolled system. Regarding the comparison between both controllers, the Skyhook-PID controller performs well for both sinusoidal and random inputs. The

performance of improvement between them is 24% for sine input and 3% for the random input. However, the performance of the PID controller has been demonstrated to be the best controller when the system is subjected to a step input disturbance.

Table 5. Analysis metric for each system at varies input.

Input	System	RMS	Percentage of Improvement
Step	Passive	1.00×10^{-2}	-
	PID	6.98×10^{-6}	99.93%
	Skyhook-PID	1.66×10^{-4}	98.34%
Sine	Passive	3.86×10^{-3}	-
	PID	9.58×10^{-4}	75.18%
	Skyhook-PID	4.35×10^{-5}	98.87%
Random	Passive	1.43×10^{-3}	-
	PID	1.16×10^{-4}	91.89%
	Skyhook-PID	7.27×10^{-5}	94.92%

5. Conclusion

A commercial software called Algodoos serves as a no-cost 2D physics simulation tool for verifying the railway pantograph model in vertical directions. The chosen 3DOF model with lumped mass proves to be an effective means of capturing the physical attributes of the actual pantograph. The outcomes provide a comprehensive and clear explanation of the real pantograph's vertical contact strip displacement, as indicated by the mean absolute relative error in both the Algodoos simulation and the MATLAB/Simulink model. The simulation results show that the contact strip responses agree between MATLAB/Simulink and Algodoos models. Since the differences are very small, which are less than 1.0%, it can be concluded that the models are verified. Next, the model was also extended to implement active pantograph control by using two types of controllers PID and Skyhook-PID with a simple method used to tune the PID controller in this system. The active controller effectively separates the effects of disturbances resulting from the wheel profile and ensures that the vertical displacement is kept constant at a level close to zero. This is demonstrated by achieving the lowest RMS value and the highest percentage improvement value. The Skyhook PID controller shows commendable performance with both sinusoidal and random disturbances with the performance improvement between both controllers being 24% for sine input and 3% for the random input. However, the performance of the PID controller has been demonstrated to be the best controller when the system is subjected to a step input disturbance with a performance improvement of as much as 2%. As a future work, the method developed can be also extended to study the other controller tuning method, higher degree-of-freedom model, and the off-line HIL testing method for the model validation process.

Acknowledgements

The authors wish to express their appreciation for the support provided by the Centre for Advanced Research on Energy (CARE) and the Universiti Teknikal Malaysia Melaka in Malacca, Malaysia through grant number PJP/2023/CARe/EV/Y00012.

Nomenclature

PID	Proportional Integral Derivative (–)
LMI	linear matrix inequalities (–)
LQR	linear quadratic regulator (–)
DOF	degree of freedom (–)
$2D$	two dimensional (–)
m	mass (kg)
k	spring stiffness (Nm^{-1})
c	damping coefficient (Ns/m)
m_1	contact strip mass (kg)
m_2	pan head mass (kg)
m_3	mass of other parts at pantograph (kg)
k_1	Spring stiffness at contact strip (Nm^{-1})
k_2	Spring stiffness at pan- head (Nm^{-1})
k_3	Spring stiffness at other parts (Nm^{-1})
c_1	damping coefficient at contact strip (Ns/m)
c_2	damping coefficient pan- head (Ns/m)
c_3	damping coefficient at other parts (Ns/m)
Z_r	displacement disturbance (m)
Z_1	displacement relative to contact strip (m)
Z_2	displacement relative to pan- head (m)
Z_3	displacement relative to other parts (m)
$X_{A,i}$	set of data from Algodoo model (–)
$X_{M,i}$	set of data from MATLAB model (–)
n	set of variables (–)
f_a	force of an actuator (N)
K_P	proportional gain tuning parameter (–)
K_I	integral gain tuning parameter (–)
K_D	derivative gain tuning parameter (–)
N	Filter coefficient (–)
c_{sky}	damping coefficient skyhook (Ns/m)
F_{sky}	control force applied to a sprung mass (N)

Greek symbols

ξ	damping ratio (–)
ξ_1	damping ratio at contact strip (–)
ξ_2	damping ratio at pan- head (–)
ξ_3	damping ratio at other parts (–)
ε_i	error (–)
$\bar{\varepsilon}$	mean relative absolute error
2π	period (rad)
α	magnitude of the control gain (–)

References

- 1) H. Duan, R. Dixon, and E. Stewart, “A disturbance observer based lumped-mass catenary model for active pantograph design and validation,” *Vehicle System Dynamics*, **61** (6) 1565–1582 (2023). doi:10.1080/00423114.2022.2085586.
- 2) J. Zhang, H. Zhang, B. Song, S. Xie, and Z. Liu, “A new active control strategy for pantograph in high-speed electrified railways based on multi-objective robust control,” *IEEE Access*, **7** 173719–173730 (2019). doi:10.1109/ACCESS.2019.2955985.
- 3) L. Koutsoloukas, N. Nikitas, and P. Aristidou, “Passive, semi-active, active and hybrid mass dampers: a literature review with associated applications on building-like structures,” *Developments in the Built Environment*, **12** (2022). doi:10.1016/j.dibe.2022.100094.
- 4) P. Nāvīk, S. Derosa, and A. Rønning, “Development of an index for quantification of structural dynamic response in a railway catenary section,” *Eng Struct*, **222** (November 2019) 111154 (2020). doi:10.1016/j.engstruct.2020.111154.
- 5) J. Ko, N. Takata, K. Thu, and T. Miyazaki, “Dynamic modeling and validation of a carbon dioxide heat pump system,” *Evergreen*, **7** (2) 172–194 (2020). doi:10.5109/4055215.
- 6) B. Gregorcic, and M. Bodin, “Algodoo: a tool for encouraging creativity in physics teaching and learning,” *Physics Teacher*, **55** (1) 25–28 (2017). doi:10.1119/1.4972493.
- 7) E. Euler, C. Prytz, and B. Gregorcic, “Never far from shore: productive patterns in physics students’ use of the digital learning environment Algodoo,” *Phys Educ*, **55** (4) (2020). doi:10.1088/1361-6552/ab83e7.
- 8) G. Poetsch, J. Evans, R. Meisinger, W. Kortüm, W. Baldauf, A. Veitl, and J. Wallaschek, “Pantograph/catenary dynamics and control,” *Vehicle System Dynamics*, **28** (2–3) 159–195 (1997). doi:10.1080/00423119708969353.
- 9) S.R. Marjani, and D. Younesian, “Active vibration control for the mitigation of wheel squeal noise based on a fuzzy self-tuning pid controller,” *Shock and Vibration*, **2022** (2022). doi:10.1155/2022/3978230.
- 10) Z. Peng, and S. Zhou, “Mechanical characteristics and vibration control of railway signal relay,” *Recent Advances in Electrical and Electronic Engineering*, **16** (6) 654–663 (2023). doi:10.2174/2352096516666230412085756.
- 11) M.F. Farhan Kamerul Bieza, N.S.A. Shukor, M.A. Ahmad, M.H. Suid, M.R. Ghazaliv, and M.F.B.M. Jusof, “A simplify fuzzy logic controller design based safe experimentation dynamics for pantograph-catenary system,” *Indonesian Journal of Electrical Engineering and Computer Science*, **14** (2) 903–911 (2019). doi:10.11591/ijeecs.v14.i2.pp903-911.
- 12) H. Wang, Z. Han, Z. Liu, and Y. Wu, “Deep reinforcement learning based active pantograph

- control strategy in high-speed railway,” *IEEE Trans Veh Technol*, **72** (1) 227–238 (2023). doi:10.1109/TVT.2022.3205452.
- 13) B. Wang, S. Wen, and Y. Shen, “LQR active control of fractional-order pantograph-catenary system based on feedback linearization,” *Math Problem Eng*, **2022** 1–11 (2022). doi:10.1155/2022/2213697.
 - 14) X. Lu, H. Zhang, Z. Liu, F. Duan, Y. Song, and H. Wang, “Estimator-based h_{∞} control considering actuator time delay for active double-pantograph in high-speed railways,” *Journal of Low Frequency Noise Vibration and Active Control*, **40** (1) 442–457 (2021). doi:10.1177/1461348419876791.
 - 15) T.-C. Lin, C.-W. Sun, Y.-C. Lin, and M.M. Zirkohi, “Intelligent contact force regulation of pantograph-catenary based on novel type-reduction technology,” *Electronics (Switzerland)*, **11** (1) (2022). doi:10.3390/electronics11010132.
 - 16) Y. Song, T. Jiang, P. Nāvik, and A. Rønquist, “Geometry deviation effects of railway catenaries on pantograph-catenary interaction: a case study in norwegian railway system,” *Railway Engineering Science*, **29** (4) 350–361 (2021). doi:10.1007/s40534-021-00251-0.
 - 17) N.A. Al-Awad, I.K. Abboud, and M.F. Al-Rawi, “Genetic algorithm-pid controller for model order reduction pantographcatenary system,” *Applied Computer Science*, **17** (2) 28–39 (2021). doi:10.23743/acs-2021-11.
 - 18) M. Ibrahim, M.A. Abdullah, M.H. Harun, F. Mohamed Jamil, and F. Ahmad, “Active displacement control of pantograph-catenary system for a half-body railway model,” *Periodica Polytechnica Transportation Engineering*, (2024). doi:10.3311/PPtr.23285.
 - 19) M.A. Abdullah, A. Ibrahim, Y. Michitsuji, and M. Nagai, “Active control of high-speed railway vehicle pantograph considering vertical body vibration,” *International Journal of Mechanical Engineering and Technology (IJMET)*, **4** (6) 263–274 (2013).
 - 20) P. Zdziebko, A. Martowicz, and T. Uhl, “An investigation on the active control strategy for a high-speed pantograph using co-simulations,” *Proceedings of the Institution of Mechanical Engineers. Part I: Journal of Systems and Control Engineering*, **233** (4) 370–383 (2019). doi:10.1177/0959651818783645.
 - 21) J. Ros, and S. Lain, “PID Controller Tuning in Tram Pantograph Systems,” 2020. <https://hal.archives-ouvertes.fr/hal-02977763>.
 - 22) C. Liu, L. Chen, X. Yang, X. Zhang, and Y. Yang, “General theory of skyhook control and its application to semi-active suspension control strategy design,” *IEEE Access*, **7** 101552–101560 (2019). doi:10.1109/ACCESS.2019.2930567.
 - 23) S.B.A. Kashem, S. Roy, and R. Mukharjee, “A modified skyhook control system (SKDT) to improve suspension control strategy of vehicles,” in: 2014 International Conference on Informatics, Electronics & Vision (ICIEV), 2014: pp. 1–8. doi:10.1109/ICIEV.2014.6850696.
 - 24) M.H. Harun, W.M.Z.W. Abdullah, H. Jamaluddin, R.A. Rahman, and K. Hudha, “Hybrid skyhook-stability augmentation system for ride quality improvement of railway vehicle,” in: *Applied Mechanics and Materials*, Trans Tech Publications Ltd, 2014: pp. 141–145. doi:10.4028/www.scientific.net/AMM.663.141.
 - 25) M.H. Harun, M.A. Abdullah, S. Anuar, A. Bakar, M. Zakaria, and M. Nasir, “Railway vehicle stability improvement using bogie-based skyhook control,” in: *Proceedings of Mechanical Engineering Research Day*, 2020: pp. 41–42.
 - 26) F.M. Jamil, M.A. Abdullah, M.H. Harun, M. Ibrahim, F. Ahmad, and U. Ubaidillah, “Analysis of active secondary suspension with modified skyhook controller to improve ride performance of railway vehicle,” *J Teknol*, **85** (5) 43–54 (2023). doi:10.11113/jurnalteknologi.v85.19771.